Journal of Geoscience and Environment Protection, 2024, 12, 1-19
https://www.scirp.org/journal/gep
ISSN Online: 2327-4344
ISSN Print: 2327-4336

Geospatial and Statistical Analysis of Land Surface Temperature and Land Surface Characteristics of Jaipur and Ahmedabad Cities of India

Rupesh Kumar Gupta

Department of Continuing Education and Extension, Faculty of Social Science, University of Delhi, Delhi, India
Email: gisrs2004@gmail.com

How to cite this paper: Gupta, R. K. (2024). Geospatial and Statistical Analysis of Land Surface Temperature and Land Surface Characteristics of Jaipur and Ahmedabad Cities of India. *Journal of Geoscience and Environment Protection, 12,* 1-19.
https://doi.org/10.4236/gep.2024.128001

Received: June 23, 2024
Accepted: July 29, 2024
Published: August 1, 2024

Abstract

Land surface temperature (LST) is a phenomenon that significantly affects the environment, the cities' liveability, and the citizens' well-being. This Study aims to perform a comparative study of the microclimate and Surface Urban Heat Island (SUHI) phenomenon of two metropolitan cities of India, i.e. Jaipur and Ahmedabad, using MODIS Satellite data, whereas Landsat Data was used to analyse the Land Surface Characteristics by an index-based approach. The Study's findings reveal that Ahmedabad has 35.53 per cent of the total area classified as having a low potential, and 13.55 per cent is designated as a high potential LST zone. Meanwhile, in Jaipur, 30.45 per cent of the city's total area is identified as a low potential LST zone and 12.69 per cent as a high potential LST zone. This Study highlights the importance of mitigating the UHI phenomenon in urban centres for the overall well-being of city dwellers. It will help policymakers and stakeholders comprehend plans and take initiatives to minimise the effects of the UHI phenomenon on rapidly growing cities.

Keywords

LST, UHI, Index-Based Approach, Built-Up, Remote Sensing, GIS

1. Introduction

Urbanisation is one of the most important human endeavours affecting regional and local ecologies and the environment globally (Nasir et al., 2022; Rendana et al., 2023; Turner et al., 1990). It is the main factor converting naturally occurring surface areas into impermeable surfaces that humans produce. There are no-

ticeable climate changes brought about by introducing materials with different albedos. The atmosphere and surface are altered by urbanisation, producing a thermal temperature that is noticeably warmer than that of neighbouring rural areas, especially at night. This phenomenon is an urban heat island (UHI) (Voogt & Oke, 2003).

Urban heat islands are a significant aspect of urban climates, impacting the well-being of inhabitants and the environment. It has become a global phenomenon with an increasing population in the urban centres (Sannigrahi et al., 2017; Chudnovsky et al., 2004; Singh & Grover, 2014). Urbanisation has changed the cities' landscapes, significantly altering the biophysical environment and the heat balance (Lo & Quattrochi, 2003; Li et al., 2018). These landscape modifications have resulted in converting natural pervious surfaces like agricultural land and green cover into built-up areas (Swamy et al., 2017; Carlson & Arthur, 2000; Gupta, 2024). The transformations in Land Use and Land Cover (LULCs) of the urban environments give rise to many issues like urban sprawl (Sundarakumar et al., 2012; Subramani & Vishnumanoj, 2014; Rahman et al., 2011), water scarcity (Fuentes et al., 2021; Menzel et al., 2009), housing problems (Desalegn et al., 2014; Haffner & Hulse, 2019), microclimatic variations and formation of Urban Heat Island (Fashae et al., 2020; Lo & Quattrochi, 2003; Gupta & Parashar, 2020). An Urban Heat Island is a phenomenon where the urban areas experience higher temperatures than their adjacent countryside (Najafzadeh et al., 2021; Liu & Zhang, 2011). The intensity of the urban heat island varies spatially and temporally, with economic activities in metropolitan areas contributing significantly to its formation (Tang, 2022). Several factors are also responsible for creating and intensifying the UHI effect in the cities, like the presence of vegetation and water bodies, local weather, heat emissions, and building geometry (Gupta, 2012; Voogt & Oke, 2003).

The UHI is broadly categorised into Surface Urban Heat Island (SUHI) and Atmospheric Urban Heat Island (AUHI). SUHI is more pronounced during the summer (Valsson & Bharat, 2009), while AUHI is more prominent at night and in winter (Chen et al., 2006). A direct relationship exists between surface and atmospheric temperatures, particularly within the canopy layer. Forested areas, vegetated landscapes, and water bodies often exhibit cooler surface temperatures, contributing to lower atmospheric temperatures in those locales. Conversely, dense built-up zones and extensive concrete areas tend to have warmer surface temperatures, which can lead to elevated atmospheric temperatures in those urban environments (Singh & Grover, 2014).

The quantitative characterization of degraded land was achieved through the application of the Normalized Difference Barren Index (NDBaI) and the Modified Normalized Difference Water Index (MNDWI) (Gao, 1996; Zha et al., 2003). The LST was compared to the normalized difference vegetation index (NDVI), NDBaI, and MNDWI in order to assess the ambient environmental status for living organisms (Sun et al., 2012). Vegetation-based indicators offer a means of demonstrating the quantity and quality of vegetation cover (Moisa et al., 2022;

Jiang & Tian, 2010).

Assessment of the geographical flexibility of the NDVI, LST, NDBaI, and MNDWI is crucial for natural resource monitoring and decision-making in natural and environmental research (Zareie et al., 2016). According to Yuan and Bauer (2007), the significance of displaying the distribution of green space has also been validated by using the NDVI. Moreover, a number of studies have reported that the expansion of agricultural and grazing land, urbanization, deforestation, and forest fires were the primary factors contributing to the steady decrease in remote sensing indices such as MNDWI and NDVI, which in turn caused increases in NDBaI and LST (Zhou & Wang, 2010; Mimbrero et al., 2014).

Based on an index-based approach, this study allows for a deeper understanding of the interaction between LST and UHI and their relationship with UTFVI, NDVI, NDBI, NDBal, and MNDWI. Although the UHI effect has been extensively investigated in other cities, more is needed to know about the surface UHI effect and various index-based approaches. This study fills this gap in the literature and clarifies the UHI effect in a rapidly growing metropolitan area in India.

For this purpose, we have selected two planned cities in India. Jaipur is called the Pink City of India, and Ahmedabad is called the Manchester of India. Both metropolitan cities have different histories: Ahmedabad is primarily known for its textile sector, while Jaipur is India's most visited tourist destination. Ahmedabad is situated in the western part of India, while Jaipur is in the northwest part of the country.

The study dramatically advances our understanding of the topic and provides a unique perspective on the impact of urban heat islands (UHIs) and their effects on urban microclimates and habitats. The current study aims to evaluate the patterns and dynamics of LST, SUHI, and relation to geospatial indices (UTFVI, NDVI, NDBI, NDBal and MNDWI) of two metropolitan cities. To develop a map using index based method to investigate the connection between LST and above geospatial indices. This approach contributes to understanding how urban heat island (UHI) affects altered development levels, land-use patterns, and urban landscapes of the city. In addition, the study broadens our understanding of the local consequences of LST and UHI, which will assist policymakers and urban planners in developing workable plans to mitigate the detrimental effects of UHI on public health and urban environments.

2. Material and Methods

2.1. Study Area

Jaipur, the capital city of the north western Indian state of Rajasthan, is surrounded by fertile plains, hills, and desert areas. The Aravalli Mountains enclose the city from three sides and serve as natural protection for the city. The city is at an average elevation of 432 meters above the mean sea level and has a semi-arid climate with hot summers and mild winters as characteristic features. With a

population of approximately 2.8 million (Census of India, 2011), the city is an intrinsic example of proper urban planning and development (Figure 1).

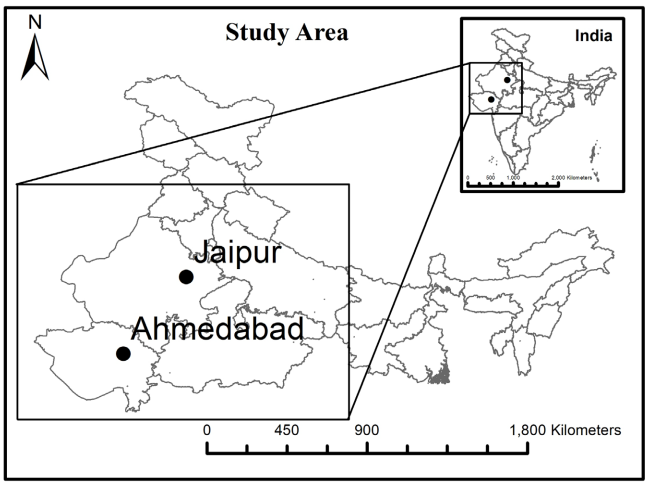

Figure 1. Location map. Source: By author using GIS.

Ahmedabad, an economic and financial hub in the western state of Gujarat, is known for its varied geographical features. The city is located on the banks of the Sabarmati River, with the landscape composed of flat fields and undulating terrain with an average elevation of 50 meters above the mean sea level. Ahmedabad has a semi-arid climate characterised by hot summers and mild winters. Arid landscapes characterise the city's surroundings, and industrial areas and agricultural zones dominate its suburbs. With an approximate population of 5.5 million (Census of India, 2011), Ahmedabad is famous for historical events, economic dynamism, and urban development (Figure 1).

Jaipur and Ahmedabad, located in the western part of India, are experiencing hot summers and mild winters. The rugged Aravali hills surround Jaipur, while Ahmedabad is situated along the banks of the Sabarmati River. Ahmedabad's average summer maximum is 39˚C, and average minimum is 24˚C while in winter, the average maximum temperature is 30˚C, and the average minimum is 15˚C. For Jaipur, in summer, the average maximum temperature is 40.1˚C, and the average minimum is 25.3˚C whereas in winter, the average maximum temperature is 22.6˚C, and the average minimum goes down to 7.9˚C. Ahmedabad is called the "Manchester of India" due to its thriving textile industry, whereas Jaipur also encompasses industries like Cotton textile, leather, mineral-based, wooden, etc. Both the cities are enriched with cultural heritage and historical significance.

2.2. Datasets

The current study's data sources primarily involved using geospatial data in the form of satellite images. The satellite images of the Landsat 8 OLI, TIRS, and MODIS Terra Sensors were acquired from the USGS Earth Explorer and NASA Earth Data platforms. The details of the Data acquired are given in Table 1.

Table 1. Datasets used.

S. No	Satellite	Spatial Resolution	Sensor	Time	Source
1	Landsat 8	30 m	OLI & TIRS	June 2023	USGS Earth Explorer
2	MODIS	1 km	Terra	June 2023	NASA Earth Data

Source: Open-source satellite data.

2.3. Methods

After the acquisition of the satellite data, GIS-based tools and techniques were incorporated to analyse and interpret the datasets. The MODIS Terra data was used for the calculation of the Land Surface temperatures of the cities, whereas the Landsat 8 Data were utilised for the mapping and identification of Land Surface Characteristics (Zhu & Woodcock, 2014; Huang et al., 2009; Hassan et al., 2016; Tao et al., 2018; Spruce et al., 2013; Park et al., 2019). For this purpose, the following method was used to determine the relationship between LST and several geospatial indices to assess the green urban environment. The UTFVI plays a prominent role in ecologically evaluating the Urban Environment by considering the Land Surface Temperatures (LST). The NDBI helps indicate the high built-up area, NDVI, which is the numerical indicator for evaluating the health and density of vegetation. MNDWI calculates the water concentration in vegetation canopies, and NDBaI is beneficial in identifying and mapping the areas of bare soil or exposed ground. The following indices were incorporated in the study:

2.3.1. Urban Thermal Field Variance Index (UTFVI)

The UTFVI plays a prominent role in ecologically evaluating the Urban Environment by considering the Land Surface Temperatures (LST). It considers the impact of the LST of different locations with the overall mean LST of the Urban Area. Using the Land Surface Temperatures, the UTFVI index was used to Surface Urban Heat Island (SUHI) (Sobrino & Irakulis, 2020; Toy et al., 2007; Liu & Zhang, 2011). The following equation calculates it:

$$\mathrm{UTFVI} = 1 - \left(\mathrm{LST}_{\mathrm{Mean}} / \mathrm{LST}_{\mathrm{Pixel}}\right) \quad (1)$$

LST is the land surface temperature obtained by the satellite data using MODIS Terra. $\mathrm{LST}_{\mathrm{Pixel}}$ is the Pixel value of the LST of different locations, and $\mathrm{LST}_{\mathrm{Mean}}$ is the Mean value of the whole urban area considered.

After the computation of the above indices, Area Identification and Extraction were performed to analyse Land Surface Characteristics and Urban Heat Exposure using GIS tools and Statistical techniques.

2.3.2. Normalised Difference Vegetation Index (NDVI)

The NDVI incorporates the Red and Infrared bands of the satellite data products to delineate the Vegetation cover at a particular location from its surrounding land uses (Reed et al., 1994; Huang et al., 2019; Piao et al., 2011; Mao et al.,

2012). The following Equation calculates it:

$$\text{NDVI} = \frac{\text{Near Infrared} - \text{Red}}{\text{Near Infrared} + \text{Red}}$$

$$\text{NDVI for Landsat 8} = \frac{\text{Band 5} - \text{Band 4}}{\text{Band 5} + \text{Band 4}} \quad (2)$$

2.3.3. Normalised Difference Built-Up Index (NDBI)

The NDBI utilises the middle and near-infrared ranges to differentiate the built-up areas from other features. The following equation calculates it (Zha et al., 2003):

$$\text{NDBI} = \frac{\text{Short wave Infrared} - \text{Near InfraRed}}{\text{Short wave Infrared} + \text{Near InfraRed}}$$

$$\text{NDBI for Landsat 8} = \frac{\text{Band 6} - \text{Band 5}}{\text{Band 6} + \text{Band 5}} \quad (3)$$

2.3.4. Modified Built-Up Index (MBI)

An improved and modified approach (He & Reith, 2023) gives better results for extracting the Built-Up Land and is calculated by the following equation:

$$\text{Modified NDBI} = \text{NDBI} - \text{NDVI} \quad (4)$$

2.3.5. Normalised Difference Bareness Index (NDBaI)

The NDBaI utilises the Middle-range Infrared and Thermal range bands to extract the Bare Land from the surrounding areas (Zhou et al., 2014). The following equation calculates it:

$$\text{NDBaI} = \frac{\text{Short wave Infrared} - \text{Thermal}}{\text{Short wave Infrared} + \text{Thermal}}$$

$$\text{NDBaI for Landsat 8} = \frac{\text{Band 6} - \text{Band 10}}{\text{Band 6} + \text{Band 10}} \quad (5)$$

2.3.6. Modified Normalised Difference Water Index (MNDWI)

The MNDWI proves to be more effective in improving and extracting water-related information from within the nearby built-up environment or other land uses as it can minimise or eliminate noise from built-up land, a feature that sets it apart from the NDWI (Xu, 2006). The following equation calculates it:

$$\text{MNDWI} = \frac{\text{Green} - \text{Short wave Infrared}}{\text{Green} + \text{Short wave Infrared}}$$

$$\text{MNDWI for Landsat 8} = \frac{\text{Band 3} - \text{Band 6}}{\text{Band 3} + \text{Band 6}} \quad (6)$$

3. Results and Discussion

3.1. Land Surface Temperatures

The Thermal band data acquired by the satellite sensors is generally utilised to study the Land Surface temperatures. The Brightness values measured are converted into the Temperature values using the following equation in GIS Software:

$$\text{Temperature in } ^\circ\text{C} = \text{DN} * 0.02 - 273.15$$

where DN stands for the Digital Number of the MODIS Land Surface Temperature Satellite Data Product.

The calculated results of LST (Figure 2) reveal that in Ahmedabad, the maximum recorded LST stands at 45.19˚C, while the minimum is 37.31˚C, resulting in a temperature range of 7.88˚C. Similarly, Jaipur exhibits slightly higher temperatures, with a maximum LST of 45.51˚C and a minimum of 37.17˚C, resulting in a slightly wider temperature range of 8.34˚C (Figure 3).

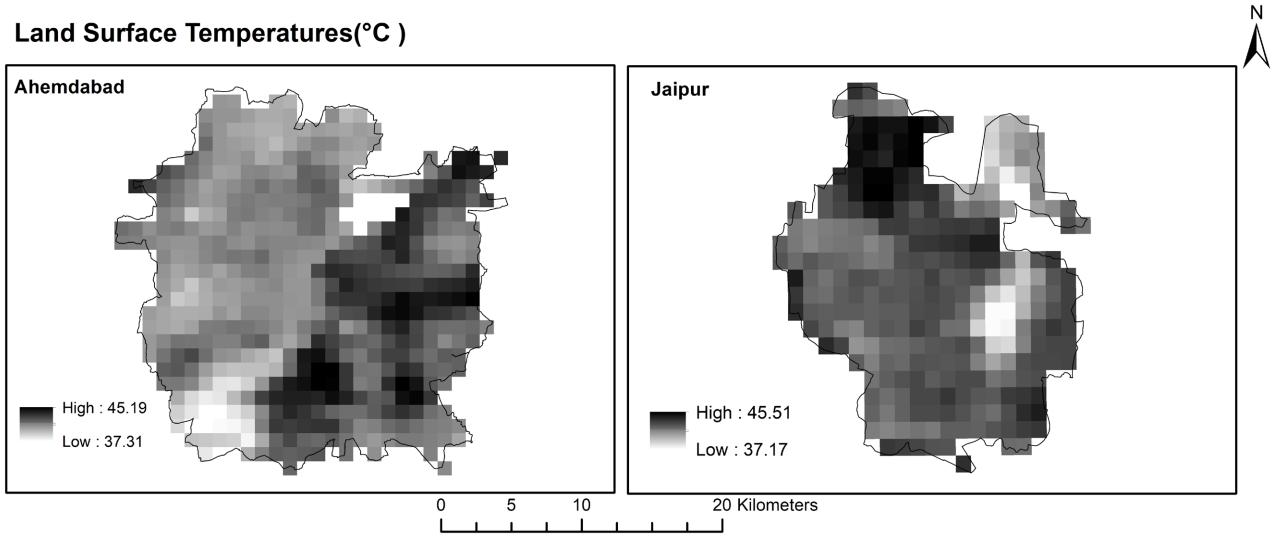

Figure 2. Land surface temperature map. Source: Open-source satellite data.

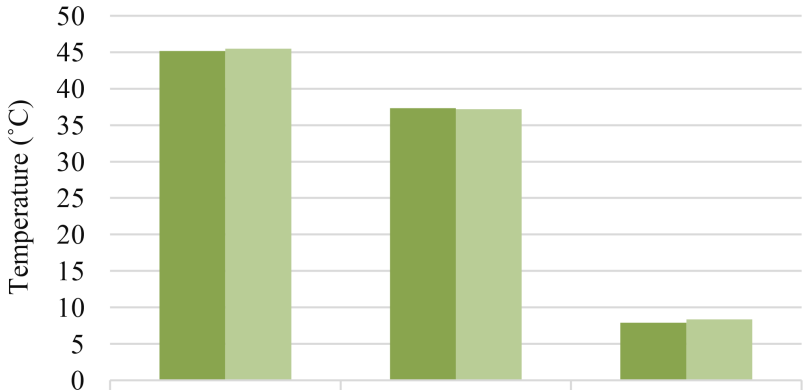

	LST-Maximum (in ˚C)	LST-Minimum (in ˚C)	Range (in ˚C)
Ahmedabad	45.19	37.31	7.88
Jaipur	45.51	37.17	8.34

Figure 3. Maximum & minimum values of LST. Source: Open-source Satellite data.

3.2. Surface Urban Heat Island

The UTFVI was used to analyse the spatial patterns of the SUHI in both cities. When the UTFVI was calculated, the values were reclassified into high, medium, and low UHI potential zones (Figure 4).

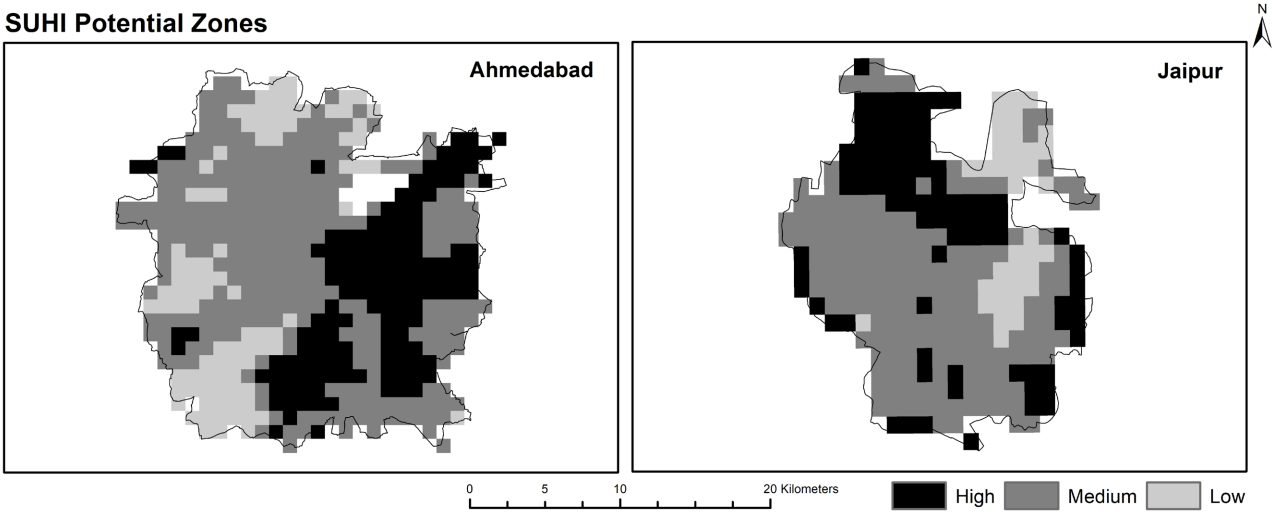

Figure 4. Surface urban heat island map. Source: Open-source Satellite data.

In Ahmedabad, the analysis reveals that 35.53 per cent of the total area is classified as having a low potential for UHI formation, while 50.92 per cent falls within the moderate potential category, and 13.55 per cent is designated as a high potential UHI zone. Similarly, in Jaipur, 30.45 per cent of the city's total area is identified as a low potential UHI zone, with 56.86 per cent categorized as moderate potential and 12.69 per cent classified as a high potential UHI zone (Figure 5).

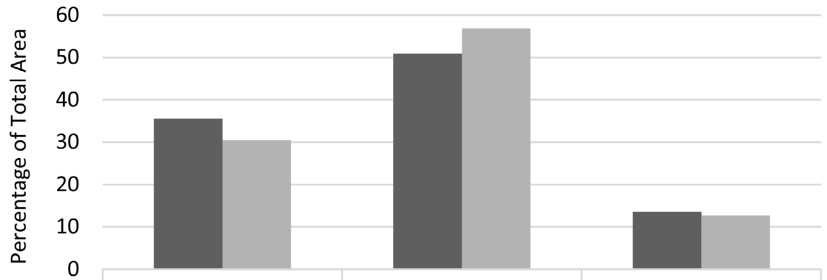

	Low Potential UHI Zone	Moderate Potential UHI Zone	High Potential UHI Zone
Ahmedabad	35.53	50.92	13.55
Jaipur	30.45	56.86	12.69

Figure 5. Area Statistics of SUHI. Source: Open-source satellite data.

In Ahmedabad, areas characterized by high potential UHI include industrial zones along the city's eastern parts, the Old City area, Khadia, and certain peri-urban regions primarily consisting of barren land towards the southern outskirts. Conversely, locations with low potential UHI zones are generally found along the Sabarmati River, peri-urban regions, and surrounding waterbodies such as Kankaria Lake and Chandola Lake. On the other hand, in Jaipur, high-potential UHI zones are predominantly found in industrial areas in the northwest part of the city and specific localities like Shastrinagar and Bapu Bazar. On the other

hand, areas with low potential for UHI development in Jaipur include regions characterized by dense vegetation, such as those surrounding Jal Mahal, Jhalana Safari Park, the Aravali Mountains, and Central Park (Table 2).

Table 2. Major locations of Urban Heat Island (UHI).

City	High Potential UHI Zones	Low Potential UHI Zones
Ahmedabad	Industrial areas along the eastern parts of the city, Old City, Khadia, and some peri-urban in the form of barren land towards the south of the city	Areas along the Sabarmati River and a few peri-urban areas of the city, areas around Kankaria Lake, Chandola Lake, etc.
Jaipur	Industrial Areas in the Northwest part of the city, Shastrinagar, Bapu Bazar, etc.	Dense Vegetation around Jal Mahal, Jhalana Safari Park, Aravali Mountains, Central Park, etc.

Source: Open-source satellite data.

3.3. Land Surface Characteristics

3.3.1. Vegetation

The values obtained through Normalised Difference Vegetation Index (NDVI) Mapping (Figure 6) reveal the information about the vegetation cover in Ahmedabad and Jaipur, ranging from a maximum of 0.560 to a minimum of −0.072 in Ahmedabad and from a maximum of 0.550 to a minimum of −0.069 in Jaipur. Both cities display certain areas with dense vegetation, with Ahmedabad showing slightly higher NDVI values than Jaipur (Table 3).

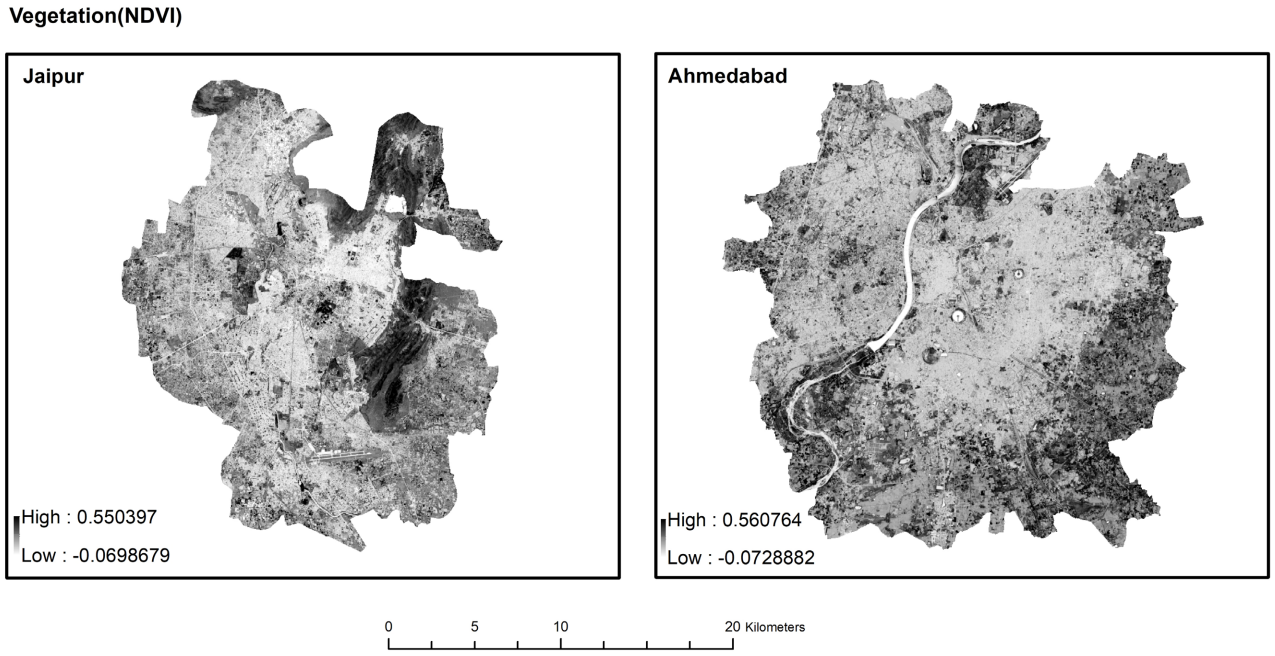

Figure 6. Vegetation-NDVI Map. Source: Open-source satellite data.

Table 3. Values of Normalised Difference Vegetation Index (NDVI).

	Ahmedabad		Jaipur	
	Maximum	Minimum	Maximum	Minimum
NDVI	0.560	−0.072	0.550	−0.069

Source: Open-source satellite data.

The area statistics reveal that approximately 26.77 per cent of Ahmedabad's total area is covered by high vegetation. This vegetation is predominantly found along the Sabarmati River, spanning the city's northern and southern parts. This greenery contributes to biodiversity and environmental health by improving air quality and mitigating the urban heat island effect. On the other hand, Jaipur's healthy vegetation covers a slightly more significant portion, accounting for 25.39 per cent of the total area. In Jaipur, this vegetation is concentrated around the Aravali Mountains, a significant geographical feature of the region. Additionally, dense vegetation is found in and around the areas like Jal Mahal, Jhalana Safari Park, and Central Park (Table 7).

3.3.2. Built-Up Area

Upon mapping the areas of Built-up areas through MBI, the values highlight the extent of urbanization in Ahmedabad and Jaipur (Figure 7). The values range from a maximum of 0.318 to a minimum of −0.930 in Ahmedabad, and from a maximum of 0.291 to a minimum of −0.932 in Jaipur; both cities exhibit considerable built-up areas (Table 4). This suggests that urban development and infrastructure expansion have significantly altered the land cover in both cities, leading to increased impervious surfaces and reduced vegetated areas.

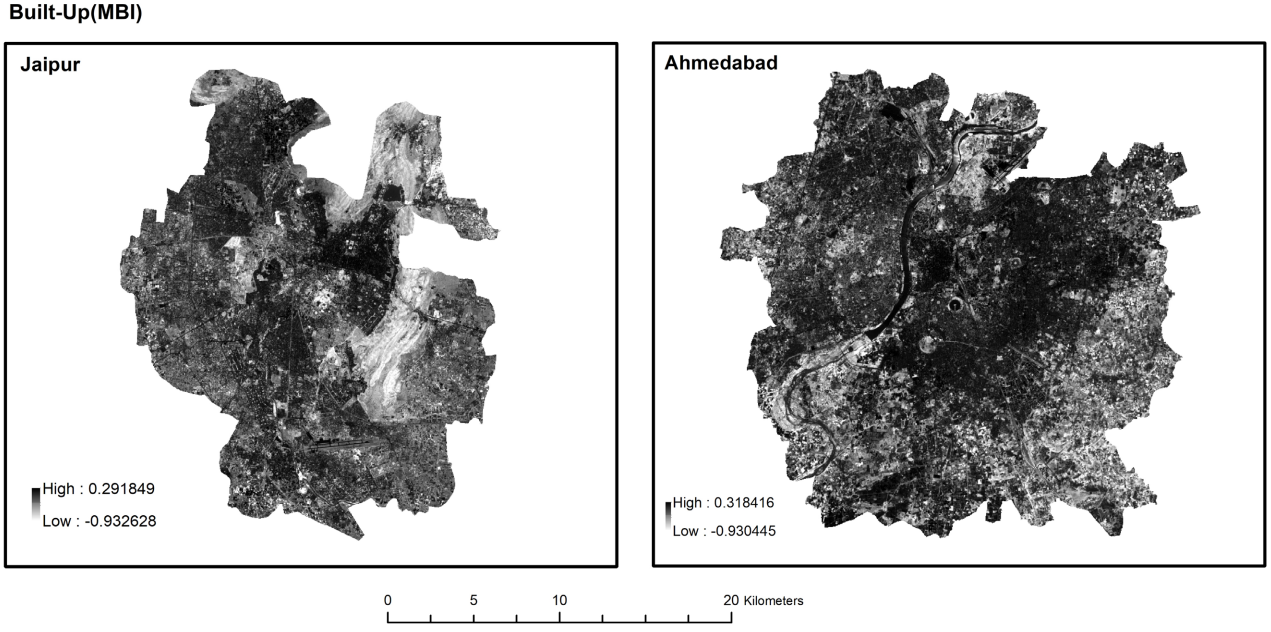

Figure 7. Modified Built-up Index (MBI) Map. Source: Open-Source Satellite data.

Table 4. Values of Modified Built-up Index (MBI).

	Ahmedabad		Jaipur	
	Maximum	Minimum	Maximum	Minimum
MBI	0.318	−0.930	0.291	−0.932

Source: Open-source satellite data.

Most of Ahmedabad's urban landscape is covered by built-up areas, accounting for 56.14 per cent of the total geographical area. These areas include densely populated neighbourhoods such as Dariyapur, Saraspur, Kalupur, the Old City, Khadia, and Asarwa. Meanwhile, in Jaipur, high-built areas cover about 50.83 per cent of Jaipur's total geographical area. These areas include Shastrinagar, Bapu Bazar, Laxminarayan Puri, Subhash Chowk, and Sundarvihar (Table 7).

3.3.3. Water Bodies

The values obtained by the MNDWI mapping indicate the spatial cover of water bodies in both cities (Figure 8). The values range from a maximum of 0.347 to a minimum of −0.504 in Ahmedabad and from a maximum of 0.139 to a minimum of −0.516 in Jaipur; both cities display the presence of water bodies (Table 5).

Table 5. Values of Modified Normalised Difference Water Index (MNDWI) Indices.

	Ahmedabad		Jaipur	
	Maximum	Minimum	Maximum	Minimum
MNDWI	0.347	−0.504	0.139	−0.516

Source: Open-source satellite data.

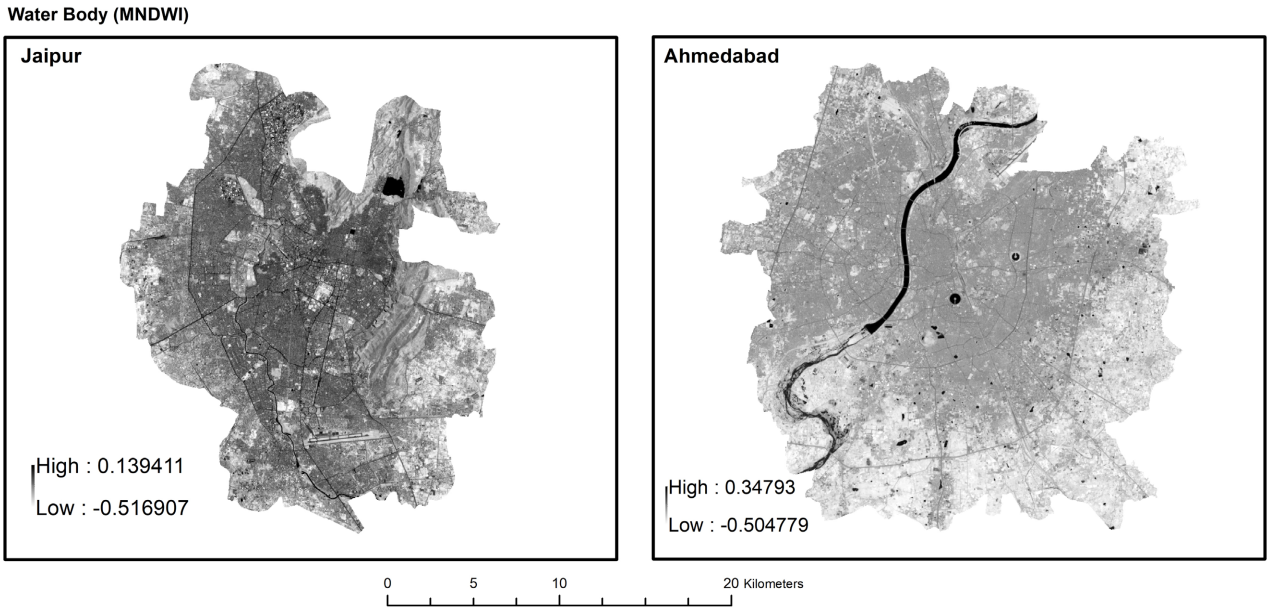

Figure 8. Modified Normalised Difference Water Index (MNDWI) Map. Source: Open-Source Satellite data.

Water bodies cover 4.64 per cent of Ahmedabad's total area, including the Sabarmati River, Kankaria Lake, Chandola Lake, Malek Saban Lake, Vanar Vat Talab, Piranha Lake, and Isanpur Lake. Jaipur has a smaller proportion of water bodies, covering only 1.21 per cent of Jaipur's total area, including significant water bodies like Jal Mahal and Amanishah Nala (Table 7).

3.3.4. Barren Land

The Normalized Difference Bareness Index (NDBaI) values detail the extent of bare land cover in Ahmedabad and Jaipur (Figure 9). The values range from a maximum of 0.252 to a minimum of −0.556 in Ahmedabad and from a maximum of 0.384 to a minimum of −0.069 in Jaipur, indicating varying degrees of bareness (Table 6).

Table 6. Values of Normalized Difference Bareness Index (NDBaI) Indices.

	Ahmedabad		Jaipur	
	Maximum	Minimum	Maximum	Minimum
NDBaI	0.252	−0.556	0.384	−0.069

Source: Open-Source Satellite data.

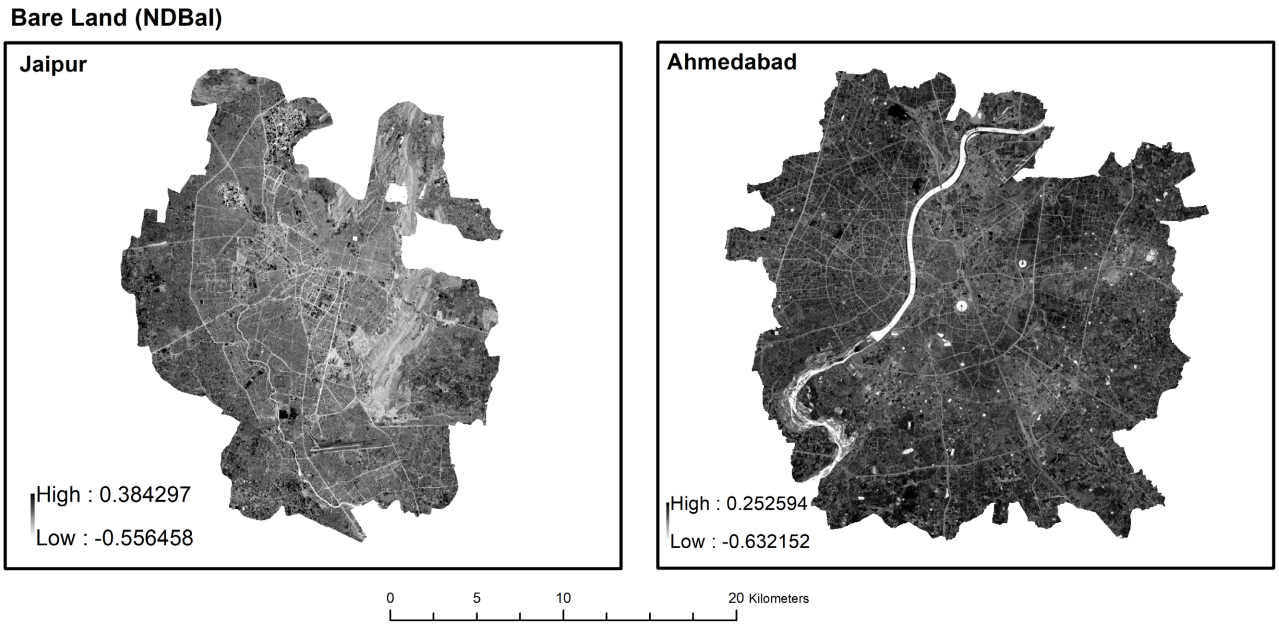

Figure 9. Normalized Difference Bareness Index (NDBaI) Map. Source: Open-Source Satellite data.

Bare land areas cover 11.30 per cent of Ahmedabad's total area, primarily in peri-urban regions surrounding the city. These areas may include undeveloped or agricultural land and patches of barren terrain. In contrast, as compared to Ahmedabad, Jaipur constitutes high bare land areas with approximately 20.34 per cent of Jaipur's total area. These areas are primarily situated in peri-urban regions in the western and southern parts of the city and around Mansarovar (Table 7).

Table 7. Area statistics of Surface Urban Heat Island (SUHI).

Land Characteristics (derived from indices)	Ahmedabad		Jaipur	
	Percentage of total area	Location	Percentage of total area	Location
High Vegetation	26.77	Areas Along the Sabarmati River in the North and South Parts of the City	25.39	Aravali Mountains, Dense Vegetation around Jal Mahal, Jhalana Safari Park, Central Park
High Built-Up	56.14	Dariyapur, Saraspur, Kalupur, Old City, Khadia, Asarwa etc.	50.83	Shastrinagar, Bapu Bazar, Laxminarayan Puri, Subhash Chowk, Sundarvihar etc.
High Waterbody	4.64	Sabarmati, Kankaria Lake, Chandola Lake, Malek Saban Lake, Vanar Vat Talab, Biranha Lake, Isanpur Lake, Ghodsar Lake, etc.	1.21	Jal Mahal, Amanishah Nala
High Bare Land	11.30	Peri-Urban Areas of The City	20.34	Peri-Urban Areas of Western and Southern City; Areas around Mansarovar etc.

Source: Open-Source Satellite data.

3.4. Discussions

The relationship between Land Surface Temperature (LST) and land surface characteristics in the cities is crucial for understanding urban heat dynamics. Both cities exhibit significant variations in land surface characteristics, with Ahmedabad boasting 26.77 per cent higher vegetation cover than Jaipur, which is slightly lower at 25.39 per cent. Areas with abundant Vegetation, such as along the Sabarmati River in Ahmedabad and around the Aravali Mountains in Jaipur, possess lower LSTs due to the cooling effects of Vegetation through transpiration and shading. Conversely, built-up areas, which constitute the majority of urban landscapes in both cities, i.e. 56.14 per cent in Ahmedabad and 50.83 per cent in Jaipur, exhibit higher LSTs. In contrast, in Ahmedabad, the high LSTs were visible in the areas of the older city, which lack the proper planning strategies, but on the other hand, the significant UHI was visible in the north western part of the city, which is primarily owned by industrial activities. Jaipur is a set example of a city that has been planned since it was established, which has ensured the green cover in the city and controlled the haphazard development. Thus, in Jaipur, only certain city pockets witness high LST, which generally include the densely populated areas with high building density. The presence of water bodies moderates surface temperatures by absorbing and storing heat, resulting in lower LSTs, such as in the regions along the Sabarmati River in Ahmedabad and regions along Jal Mahal in Jaipur, which exhibit the minimum values of LST. In contrast, regions with significant proportions of bare land, such as peri-urban areas surrounding both cities, experience higher LSTs due to increased solar radiation absorption and reduced evaporative cooling.

The present study reveals significant information about the Land Surface characteristics and their effect on the LST and microclimatic variations of the cities. The results from the open-source satellite images show that both the cities have temperature ranges of around 8 degrees Celsius. Both cities experience the UHI effect, but the difference is found in the locations of SUHI, where Jaipur has a majority of high LSTs around industrial areas, whereas Ahmedabad experiences high LST values in the city's densely built-up areas. The healthy Vegetation and presence of water bodies in both cities modify the microclimate of the cities by mitigating the UHI phenomenon and providing greater thermal comfort to the residents.

The geographical distribution of elevated land surface temperature (LST) indicates that concrete zones are becoming urban heat island types. However, any urban zone's LST can be lowered by having a lot of greenery and water features. In urban and peri urban settings, protecting green spaces and bodies of water is one of the most crucial responsibilities of planners and legislators. Cities can improve their urban thermal environment with the use of urban plans, and it is recommended that administrative authorities create a plan specific to each circumstance.

4. Conclusion

The projected increase in land surface temperature (LST) to global climate change has had a detrimental impact on the quality of life, health, and urban environment, especially in emerging nations like India and its cities. The increasing population growth of the city is driving up demand for residential houses. Consequently, this forces the government to put aside funds for private-sector investments and government-funded housing projects. Numerous changes in land usage have resulted from the rising demand for land.

The study employed pixel-based satellite data to classify the vegetation, water bodies, barren land, urban built-up land and land surface temperature in the study area. Based on the analysis, the NDVI has been widely used to indicate vegetation richness in studies of urban heat islands, which has led to the estimation of LST. By combining NDBI and MNDWI, positive correlations between NDBI and LST were found. This process also revealed that rising land surface temperatures were accompanied by a significant rise in the area's impermeable surface. The MNDWI, however, shows a negative association because water significantly reduces temperature. In conclusion, land surface temperature correlations with NDVI, NDBI, and MNDWI can be used as a signal to monitor urban regions' thermal climate.

The importance of improving our understanding of urban microclimates to mitigate the consequences of the Urban Heat Island (UHI) Effect is emphasized in this study. Urban heat island (UHI) effects can be reduced by converting urban wastelands into parks, installing green mufflers on roadways, encouraging people to plant rooftop gardens, creating vertical gardens in office and govern-

ment buildings, and utilizing sustainable building materials that absorb heat. Consequently, this will improve the citizens' quality of life. The results of this study can be used by policymakers, urban planners, and other stakeholders to help them make well-informed decisions about the analysis and mitigation of the UHI Effect, which would improve the quality of life in Indian cities.

Author Contribution

The author developed the idea and designed the study, organized the resources, gathered and analysed data, composed the article, proofread it, and granted approval.

Acknowledgements

The author thanks NASA Earth Data and the U.S. Geological Survey (USGS) for supplying the open source satellite data. We appreciate the efforts of the editors and potential reviewers.

Competing Interests

The author declares that no known competing financial interest or personal relationship appears to have influenced any of the work presented in this paper.

References

Carlson, T. N., & Traci Arthur, S. (2000). The Impact of Land Use—Land Cover Changes Due to Urbanization on Surface Microclimate and Hydrology: A Satellite Perspective. *Global and Planetary Change, 25,* 49-65. https://doi.org/10.1016/s0921-8181(00)00021-7

Census of India (2011). *Press Release: Rural-Urban Distribution of Population (Provisional).* Press Information Bureau Website. https://censusindia.gov.in/nada/index.php/catalog/42617

Chen, X., Zhao, H., Li, P., & Yin, Z. (2006). Remote Sensing Image-Based Analysis of the Relationship between Urban Heat Island and Land Use/Cover Changes. *Remote Sensing of Environment, 104,* 133-146. https://doi.org/10.1016/j.rse.2005.11.016

Chudnovsky, A., Ben-Dor, E., & Saaroni, H. (2004). Diurnal Thermal Behavior of Selected Urban Objects Using Remote Sensing Measurements. *Energy and Buildings, 36,* 1063-1074. https://doi.org/10.1016/j.enbuild.2004.01.052

Desalegn, T., Cruz, F., Kindu, M., Turrión, M. B., & Gonzalo, J. (2014). Land-Use/Land-Cover (LULC) Change and Socioeconomic Conditions of Local Community in the Central Highlands of Ethiopia. *International Journal of Sustainable Development & World Ecology, 21,* 406-413. https://doi.org/10.1080/13504509.2014.961181

Fashae, O. A., Adagbasa, E. G., Olusola, A. O., & Obateru, R. O. (2020). Land Use/Land Cover Change and Land Surface Temperature of Ibadan and Environs, Nigeria. *Environmental Monitoring and Assessment, 192,* Article No. 109. https://doi.org/10.1007/s10661-019-8054-3

Fuentes, I., Fuster, R., Avilés, D., & Vervoort, W. (2021). Water Scarcity in Central Chile: The Effect of Climate and Land Cover Changes on Hydrologic Resources. *Hydrological Sciences Journal, 66,* 1028-1044. https://doi.org/10.1080/02626667.2021.1903475

Gao, B. (1996). NDWI—A Normalized Difference Water Index for Remote Sensing of

Vegetation Liquid Water from Space. *Remote Sensing of Environment, 58,* 257-266. https://doi.org/10.1016/s0034-4257(96)00067-3

Gupta, R. (2012). Temporal and Spatial Variations of Urban Heat Island Effect in Jaipur City Using Satellite Data. *Environment and Urbanization ASIA, 3,* 359-374. https://doi.org/10.1177/0975425312473232

Gupta, R. K. (2024). Identifying Urban Hotspots and Cold Spots in Delhi Using the Biophysical Landscape Framework. *Ecology, Economy and Society—The INSEE Journal, 7,* 137-155. https://doi.org/10.37773/ees.v7i1.954

Gupta, R., & Parashar, D. (2020). Estimation of Land Surface Temperature in the Urbanized Environment Using Multi-Resolution Satellite. *Uttar Pradesh Geographical Journal, 25,* 15-28.

Haffner, M. E. A., & Hulse, K. (2019). A Fresh Look at Contemporary Perspectives on Urban Housing Affordability. *International Journal of Urban Sciences, 25,* 59-79. https://doi.org/10.1080/12265934.2019.1687320

Hassan, S. M., Edicha, J. A., & Kabiru, U. (2016). Analysis of the Pattern of Land Degradation in Okaba, Kogi State, Nigeria. *Annals of the Social Science Academy of Nigeria, No. 20,* 72-96. https://doi.org/10.36108/ssan/1502.02.0140

He, Q., & Reith, A. (2023). A Study on the Impact of Green Infrastructure on Microclimate and Thermal Comfort. *Pollack Periodica, 18,* 42-48. https://doi.org/10.1556/606.2022.00668

Huang, C., Kim, S., Song, K., Townshend, J. R. G., Davis, P., Altstatt, A. et al. (2009). Assessment of Paraguay's Forest Cover Change Using Landsat Observations. *Global and Planetary Change, 67,* 1-12. https://doi.org/10.1016/j.gloplacha.2008.12.009

Huang, X., Zhang, T., Yi, G., He, D., Zhou, X., Li, J. et al. (2019). Dynamic Changes of NDVI in the Growing Season of the Tibetan Plateau during the Past 17 Years and Its Response to Climate Change. *International Journal of Environmental Research and Public Health, 16,* Article No. 3452. https://doi.org/10.3390/ijerph16183452

Jiang, J., & Tian, G. (2010). Analysis of the Impact of Land Use/Land Cover Change on Land Surface Temperature with Remote Sensing. *Procedia Environmental Sciences, 2,* 571-575. https://doi.org/10.1016/j.proenv.2010.10.062

Li, H., Meier, F., Lee, X., Chakraborty, T., Liu, J., Schaap, M. et al. (2018). Interaction between Urban Heat Island and Urban Pollution Island during Summer in Berlin. *Science of the Total Environment, 636,* 818-828. https://doi.org/10.1016/j.scitotenv.2018.04.254

Liu, L., & Zhang, Y. (2011). Urban Heat Island Analysis Using the Landsat TM Data and ASTER Data: A Case Study in Hong Kong. *Remote Sensing, 3,* 1535-1552. https://doi.org/10.3390/rs3071535

Lo, C. P., & Quattrochi, D. A. (2003). Land-Use and Land-Cover Change, Urban Heat Island Phenomenon, and Health Implications. *Photogrammetric Engineering & Remote Sensing, 69,* 1053-1063. https://doi.org/10.14358/pers.69.9.1053

Mao, D., Wang, Z., Luo, L., & Ren, C. (2012). Integrating AVHRR and MODIS Data to Monitor NDVI Changes and Their Relationships with Climatic Parameters in Northeast China. *International Journal of Applied Earth Observation and Geoinformation, 18,* 528-536. https://doi.org/10.1016/j.jag.2011.10.007

Menzel, L., Koch, J., Onigkeit, J., & Schaldach, R. (2009). Modelling the Effects of Land-Use and Land-Cover Change on Water Availability in the Jordan River Region. *Advances in Geosciences, 21,* 73-80. https://doi.org/10.5194/adgeo-21-73-2009

Mimbrero, M., Vlassova, L., Pérez-Cabello, F., Lloveria, R., & García-Martín, A. (2014). Analysis of the Relationship between Land Surface Temperature and Wildfire Severity in a Series of Landsat Images. *Remote Sensing, 6,* 6136-6162.

https://doi.org/10.3390/rs6076136

Moisa, M. B., Dejene, I. N., Merga, B. B., & Gemeda, D. O. (2022). Impacts of Land Use/Land Cover Dynamics on Land Surface Temperature Using Geospatial Techniques in Anger River Sub-Basin, Western Ethiopia. *Environmental Earth Sciences, 81,* Article No. 99. https://doi.org/10.1007/s12665-022-10221-2

Najafzadeh, F., Mohammadzadeh, A., Ghorbanian, A., & Jamali, S. (2021). Spatial and Temporal Analysis of Surface Urban Heat Island and Thermal Comfort Using Landsat Satellite Images between 1989 and 2019: A Case Study in Tehran. *Remote Sensing, 13,* Article No. 4469. https://doi.org/10.3390/rs13214469

Nasir, M. J., Ahmad, W., Iqbal, J., Ahmad, B., Abdo, H. G., Hamdi, R. et al. (2022). Effect of the Urban Land Use Dynamics on Land Surface Temperature: A Case Study of Kohat City in Pakistan for the Period 1998-2018. *Earth Systems and Environment, 6,* 237-248. https://doi.org/10.1007/s41748-022-00292-3

Park, J., Sim, W., Park, J., & Lee, J. (2019). Object-Based Land Cover Change Detection and Landscape Structure Analysis of Demilitarized Zone in Korea. *Sensors and Materials, 31,* 3733-3748. https://doi.org/10.18494/sam.2019.2434

Piao, S., Wang, X., Ciais, P., Zhu, B., Wang, T., & Liu, J. (2011). Changes in Satellite-Derived Vegetation Growth Trend in Temperate and Boreal Eurasia from 1982 to 2006. *Global Change Biology, 17,* 3228-3239. https://doi.org/10.1111/j.1365-2486.2011.02419.x

Rahman, A., Aggarwal, S. P., Netzband, M., & Fazal, S. (2011). Monitoring Urban Sprawl Using Remote Sensing and GIS Techniques of a Fast Growing Urban Centre, India. *IEEE Journal of Selected Topics in Applied Earth Observations and Remote Sensing, 4,* 56-64. https://doi.org/10.1109/jstars.2010.2084072

Reed, B. C., Brown, J. F., VanderZee, D., Loveland, T. R., Merchant, J. W., & Ohlen, D. O. (1994). Measuring Phenological Variability from Satellite Imagery. *Journal of Vegetation Science, 5,* 703-714. https://doi.org/10.2307/3235884

Rendana, M., Idris, W. M. R., Rahim, S. A., Abdo, H. G., Almohamad, H., Al Dughairi, A. A. et al. (2023). Relationships between Land Use Types and Urban Heat Island Intensity in Hulu Langat District, Selangor, Malaysia. *Ecological Processes, 12,* Article No. 33. https://doi.org/10.1186/s13717-023-00446-9

Sannigrahi, S., Rahmat, S., Chakraborti, S., Bhatt, S., & Jha, S. (2017). Changing Dynamics of Urban Biophysical Composition and Its Impact on Urban Heat Island Intensity and Thermal Characteristics: The Case of Hyderabad City, India. *Modeling Earth Systems and Environment, 3,* 647-667. https://doi.org/10.1007/s40808-017-0324-x

Singh, R. B., & Grover, A. (2014). Remote Sensing of Urban Micro-Climate with Special Reference to Urban Heat Island Island Using Landsat Thermal Data. *Geographia Polonica, 87,* 555-5668. https://doi.org/10.7163/gpol.2014.38

Sobrino, J. A., & Irakulis, I. (2020). A Methodology for Comparing the Surface Urban Heat Island in Selected Urban Agglomerations around the World from Sentinel-3 SLSTR Data. *Remote Sensing, 12,* Article No. 2052. https://doi.org/10.3390/rs12122052

Spruce, J. P., Smoot, J. C., Ellis, J. T., Hilbert, K., & Swann, R. (2013). Geospatial Method for Computing Supplemental Multi-Decadal US Coastal Land Use and Land Cover Classification Products, Using Landsat Data and C-CAP Products. *Geocarto International, 29,* 470-485. https://doi.org/10.1080/10106049.2013.798357

Subramani, T., & Vishnumanoj, V. (2014). Land Use and Land Cover Change Detection and Urban Sprawl Analysis of Panamarathupatti Lake, Salem. *International Journal of Engineering Research and Applications, 2,* 217-227.

Sun, Q., Wu, Z., & Tan, J. (2012). The Relationship between Land Surface Temperature

and Land Use/land Cover in Guangzhou, China. *Environmental Earth Sciences, 65,* 1687-1694. https://doi.org/10.1007/s12665-011-1145-2

Sundarakumar, K., Harika, M., Begum, S. A., Yamini, S., & Balakrishna, K. (2012). Land Use and Land Cover Change Detection and Urban Sprawl Analysis of Vijayawada City Using Multitemporal Landsat Data. *International Journal of Engineering Science and Technology, 4,* 170-178.

Swamy, G., Nagendra, S. M. S., & Schlink, U. (2017). Urban Heat Island (UHI) Influence on Secondary Pollutant Formation in a Tropical Humid Environment. *Journal of the Air & Waste Management Association, 67,* 1080-1091. https://doi.org/10.1080/10962247.2017.1325417

Tang, C. F. (2022). A Study of the Urban Heat Island Effect in Guangzhou. *IOP Conference Series: Earth and Environmental Science, 1087,* Article ID: 012015. https://doi.org/10.1088/1755-1315/1087/1/012015

Tao, Y., Lan, G., She, L., Pang, L., & Feng, K. (2018). Dynamic Monitoring of Land Cover in Dongting Lake Area between 1995-2015 with Landsat Imagery. *The International Archives of the Photogrammetry, Remote Sensing and Spatial Information Sciences, 3,* 1651-1656. https://doi.org/10.5194/isprs-archives-xlii-3-1651-2018

Toy, S., Yilmaz, S., & Yilmaz, H. (2007). Determination of Bioclimatic Comfort in Three Different Land Uses in the City of Erzurum, Turkey. *Building and Environment, 42,* 1315-1318. https://doi.org/10.1016/j.buildenv.2005.10.031

Turner, B. L. I., Clark, W. C., & Kates, R. W. (1990). *The Earth as Transformed by Human Action: Global and Regional Change in the Biosphere over the Past 300 Years*. Cambridge University Press.

Valsson, S., & Bharat, A. (2009). Urban Heat Island: Cause for Microclimate Variations. Architecture—Time Space & People, April 2009, pp. 20-25. http://www.indiaenvironmentportal.org.in/files/Architecture.pdf

Voogt, J. A., & Oke, T. R. (2003). Thermal Remote Sensing of Urban Climates. *Remote Sensing of Environment, 86,* 370-384. https://doi.org/10.1016/s0034-4257(03)00079-8

Xu, H. (2006). Modification of Normalised Difference Water Index (NDWI) to Enhance Open Water Features in Remotely Sensed Imagery. *International Journal of Remote Sensing, 27,* 3025-3033. https://doi.org/10.1080/01431160600589179

Yuan, F., & Bauer, M. E. (2007). Comparison of Impervious Surface Area and Normalized Difference Vegetation Index as Indicators of Surface Urban Heat Island Effects in Landsat Imagery. *Remote Sensing of Environment, 106,* 375-386. https://doi.org/10.1016/j.rse.2006.09.003

Zareie, S., Khosravi, H., Nasiri, A., & Dastorani, M. (2016). Using Landsat Thematic Mapper (TM) Sensor to Detect Change in Land Surface Temperature in Relation to Land Use Change in Yazd, Iran. *Solid Earth, 7,* 1551-1564. https://doi.org/10.5194/se-7-1551-2016

Zha, Y., Gao, J., & Ni, S. (2003). Use of Normalized Difference Built-Up Index in Automatically Mapping Urban Areas from TM Imagery. *International Journal of Remote Sensing, 24,* 583-594. https://doi.org/10.1080/01431160304987

Zhou, X., & Wang, Y. (2010). Dynamics of Land Surface Temperature in Response to Land-Use/cover Change. *Geographical Research, 49,* 23-36. https://doi.org/10.1111/j.1745-5871.2010.00686.x

Zhou, Y., Yang, G., Wang, S., Wang, L., Wang, F., & Liu, X. (2014). A New Index for Mapping Built-Up and Bare Land Areas from Landsat-8 OLI Data. *Remote Sensing Letters, 5,* 862-871. https://doi.org/10.1080/2150704x.2014.973996

Zhu, Z., & Woodcock, C. E. (2014). Continuous Change Detection and Classification of Land Cover Using All Available Landsat Data. *Remote Sensing of Environment, 144,* 152-171. https://doi.org/10.1016/j.rse.2014.01.011